Check for updates

Carbon dots using a household cleaning liquid as a dopant for iron detection in hydroponic systems†

Robert G. Hjort, [a] Cícero C. Pola, [a] Lisseth Casso-Hartmann, [bc] Diana C. Vanegas, [bc] Eric McLamore [bd] and Carmen L. Gomes [*a]

Iron (Fe) is a required micronutrient in plants for the production of chlorophyll and transport of oxygen. A commonly used surrogate for measuring nutrient levels is the measurement of electrical conductivity or total dissolved solids, but this technique is not selective towards any particular dissolved ion. In this study, using a conventional microwave, fluorescent carbon dots (CDs) are produced from glucose and a household cleaning product and applied towards monitoring dissolved ferric iron levels in hydroponic systems through fluorescent quenching. The produced particles have an average size of 3.19 ± 0.76 nm with a relatively high degree of oxygen surface groups. When using an excitation of 405 nm, a broad emission peak is centered at approximately 500 nm. A limit-of-detection of 0.196 ± 0.067 ppm (3.51 ± 1.21 μM) with minimal interference from common heavy metal quenchers and ions found in hydroponic systems was determined. Butterhead lettuce was grown while discretely monitoring iron levels *via* the CDs for three separate weeks of growth. The CDs displayed a non-significant difference ($p > 0.05$) in performance when compared to a standard method. These results along with a simple and relatively low-cost production method make the CDs in this study a promising tool for monitoring iron levels in hydroponic systems.

Introduction

Iron (Fe) is an essential micronutrient for nearly all organisms.[1,2] In plants, iron is a required trace element for a number of vital processes including chlorophyll biosynthesis and nitrogen reduction, with deficiency leading to chlorosis, reduced crop yields, and lower nutritional quality.[3] Dietary iron deficiency is also a global human health concern and, according to the World Health Organization (WHO), is the main cause of anemia that disproportionately affects women and children.[4] Plants are an important source of iron for humans,[5] therefore monitoring iron levels for growth and nutritional quality has an indirect implication on human health. Sensitive and highly selective methods for quantifying nutrients are based on analytical techniques that are costly, require trained

[a]Department of Mechanical Engineering, Iowa State University, Ames, IA, 50011, USA. E-mail: carmen@iastate.edu; Tel: +1 515 294 1138

[b]Department of Environmental Engineering and Earth Sciences, Clemson University, Clemson, SC, 29634, USA

[c]Interdisciplinary Group for Biotechnology Innovation and Ecosocial Change (BioNovo), Universidad del Valle, Cali 76001, Colombia

[d]Agricultural Sciences Department, Clemson University, Clemson, SC, 29634, USA

† Electronic supplementary information (ESI) available: Flow chart for CDs fabrication; effects of pH on fluorescent intensity of the CDs at 25 °C; fluorescent emission curves of the CDs after 1 and 2 years of storage; fluorescent emission and quenching of the CDs using a portable spectrophotometer; and table of comparison with recently published reports on iron sensing with CDs. See DOI: https://doi.org/10.1039/d3ra01713c

technicians, and are time consuming due to sample transportation to centralized labs, and sample pretreatment. Electrical conductivity (EC) and total dissolved solids (TDS) are commonly used methods for monitoring salt (nutrient) levels in hydroponic systems.[6,7] Although these are quick and inexpensive ways to monitor nutrient levels, these methods don't provide growers with any insight on the specific levels of each nutrient in the hydroponic solution.[8] *In lieu* of monitoring, nutrient solutions may also be refreshed on a time basis according to best management practices.[9] An inexpensive, rapid, and accurate sensing system that can monitor specific ions could provide hydroponic farmers with a useful tool that allows early intervention of nutrient deficiency/excess and dosing of appropriate loads of nutrients. Such a system would optimize growing conditions for crops, potentially increasing yields, and would likely reduce overhead costs due to more efficient use of nutrient solutions.

Carbon dots (CDs) have the potential for developing such a system. CDs are semi-spherical fluorescent carbon-based nanoparticles that were first described in the scientific literature in 2004 as an incidental finding during the purification and separation of single-walled carbon nanotubes (SWCNTs) by a preparative electrophoretic method.[10] CDs possess a carbon core with various surface groups (*e.g.*, hydroxyl, carboxyl, and carbonyl), and typically show absorption from 260 to 550 nm and photoluminescence in the visible to near-infrared (NIR) range.[11] Although CDs normally have lower emission intensity

and less control over the design process, they provide a heavy-metal-free alternative to traditional semiconductor quantum dots for sensing and imaging purposes while simultaneously offering advantages of low toxicity, biocompatibility, and high water solubility.[12,13] Various top-down and bottom-up protocols have been reported for fabricating CDs using carbon precursors such as graphite,[14] citrate,[15] candle soot,[16] and sugars from various fruit juices,[17-19] among others. Examples of methods for production of CDs include laser ablation,[20,21] electrochemical,[22,23] microwave synthesis,[24-26] and hydrothermal treatments.[27-29] Since their discovery, CDs have been applied towards several sensing and imaging applications with heavy metal detection *via* fluorescent quenching being one of the most prominent. Several recent reviews have evaluated and discussed in depth the various fabrication methods and applications of CDs including those beyond sensing applications.[30-33]

In this study, a simple method for producing CDs through microwave synthesis using a common household cleaning product, Windex®, and an abundant monosaccharide, D-glucose, is reported. Ferric iron (Fe^{3+}) was shown to act as an efficient and selective photoluminescent quencher of the fluorescent CDs, which were applied to monitor iron in a deep-water culture (DWC) hydroponic system growing butterhead lettuce (*Lactuca sativa* var. *capitata* L.). The CDs size, structure, and surface chemistry were studied using transmission electron microscopy (TEM), selected area electron diffraction (SAED), and X-ray photoelectron spectroscopy (XPS), respectively. The optical properties were characterized by measuring the absorbance, emission, fluorescent lifetime, and quantum yield. The CDs were able to monitor ferric iron in hydroponic solutions for three separate weeks of growth with statistically non-significant difference ($p > 0.05$) in performance when compared to Inductively Coupled Plasma Optical Emission Spectroscopy (ICP-OES) analysis. The obtained results show that the CDs can act as an efficient sensor for iron (Fe^{3+}), providing the opportunity to develop a relatively inexpensive and selective alternative to traditional methods used to quantify nutrient levels in hydroponic systems.

Methods and materials

Materials

Anhydrous D-glucose was purchased from Acros Organics (Geel, Belgium). Original formula Windex® (S.C. Johnson, Wisconsin, USA) and a 20 L microwave (Hamilton Beach, 1000 W) were purchased from a local supplier. Britton Robinson buffer, phosphate-buffered saline (PBS), HEPES buffer, NaOH, mercury(I) nitrate, and nitric acid were purchased from Fisher Scientific (Thermo Fisher Scientific, Massachusetts, USA). Fluorescein, iron(III) chloride, and all other salts used for interferent testing were purchased from Millipore Sigma (Darmstadt, Germany). A Hydrofarm Root Spa 8 DWC hydroponic system (HydroFarm, California, USA), 250 W full spectrum Pro Series P2500 LED light (ViparSpectra, California, USA), EC meter (HoneForest Model YL-TDS2-A, United States), pH meter, and hydroponic nutrient solutions with chelated iron (Fe-EDDHA) were purchased from an online supplier. Lettuce

seeds, rockwool germination cubes, and clay pebble growing media were purchased from a local nursery supplier.

Fabrication of CDs

The fluorescent CDs were synthesized by a one-step microwave pyrolysis method (Fig. S1†). First, stock concentration Windex® (1.180 mL) was mixed with anhydrous D-glucose (16.560 mL, 200 mM) in a tightly closed Fisher brand screw-cap glass vial (20 mL). The vial was placed near the center of the microwave (with the rotating plate removed) and treated at 50% power for ~60–65 seconds. The process was stopped once the originally transparent liquid sustained boiling and began to change into a light brown color. The container was removed and allowed to cool to room temperature for approximately 1 h. Afterwards, 1% (v/v) of KCl (1 mM) was added and the solution was filtered through a 0.2 μm surfactant-free cellulose acetate (SFCA) syringe filter (Corning, AZ, USA). All solutions, unless otherwise noted, were made with high purity water (18.23 MΩ cm).

Characterization of CDs

A PerkinElmer LS55 spectrophotometer (PerkinElmer Inc., Massachusetts, USA) with a 10% transmission filter and 6.2 slit widths was used for all fluorescent quenching measurements at an excitation wavelength of 405 nm and an emission scan from 420 to 600 nm. Quartz crystal cuvettes (Starna Scientific, Atascadero, CA) with a 10 mm pathlength were used in all experiments. A total volume of 3 mL, with 1.5 mL of CDs, Britton Robinson buffer (pH = 8.95), and stock Fe^{3+} solution (5 mM in HNO_3) with varying ratios of the latter two to reach the desired final concentration, was used for all measurements. The same procedure was followed for Pb^{2+}, Zn^{2+}, Hg^{2+}, Cd^{2+}, Ca^{2+}, Mn^{2+}, Ni^{2+}, Cr^{3+}, Al^{3+}, Cu^{2+}, Mg^{2+}, K^+, Na^+, and Fe^{2+} (100 μM). All solutions were made in 1% (v/v) HNO_3. Emission response of the CDs was interpreted using the Stern–Volmer equation (eqn (1)):

$$\frac{F_0}{F} = K_{sv}C + 1 \tag{1}$$

where F and F_0 are the fluorescent intensity in the presence and absence of the quencher, respectively. C is the quencher concentration and K_{sv} is the Stern–Volmer constant. Transmission electron microscopy (TEM) was carried out in a JEM-2100 TEM (Jeol Ltd, Peabody, MA, USA). X-ray photoelectron spectroscopy (XPS) measurements were performed using a Kratos Amicus/ESCA 3400 (Kratos Analytical, Manchester, UK). Zeta potential and mobility measurements were obtained using a Malvern Zetasizer Ultra (Malvern Instruments, United Kingdom).

Quantum yield and fluorescent lifetime

The relative quantum yield (QY) was determined by following a published protocol[34] using fluorescein (5 ppm) in NaOH (0.1 M) as the standard and an excitation wavelength of 465 nm. The QY was calculated using eqn (2):

$$\Phi_x = \Phi_{st} \frac{F_x}{F_{st}} \frac{f_{st}}{f_x} \frac{n_x^2}{n_{st}^2} \qquad (2)$$

where, F is the integral photon flux, Φ is the quantum yield, n is the refractive index of the solvent, f is the absorption factor, and subscripts x and st represent the sample and standard, respectively. Fluorescent lifetime measurements were recorded with a Horiba DeltaFlex time correlated single photon counting fluorometer (Horiba, Ltd, Kyoto, Japan) using a 359 nm excitation source, 200 ns time range, peak preset of 10 000 counts, and emission detection at 455 nm. Lifetime measurements were interpreted using eqn (3):

$$I(t) = A + \sum B_i \exp\left(-\frac{t}{\tau_i}\right) \qquad (3)$$

where B_i is the pre-exponential and represent the fraction contribution of the indicated decay time factors and τ_i is the decay time.

Hydroponics set-up and plant growth

Deep-water culture (DWC) hydroponic systems were used to grow butterhead lettuce (*Lactuca sativa* var. *capitata* L.). Seedlings were transferred to the DWC after three weeks of germination. The plants were kept on a 12–12 light schedule with a 250 W full spectrum grow light at 30% power. The hydroponic solution was maintained at an EC of approximately 2.0 mS cm^{-1}, pH of 5.5–6.5, and temperature of 22–24 °C. Oxygen was supplied to the tanks from an external pump included with the DWC hydroponic system.

Hydroponics iron measurements

Iron detection was performed with CDs using hydroponic samples from weeks one, three, and five of growth ($n = 3$ for each week) that were filtered through a 0.2 μm SFCA syringe filter (Corning, AZ, USA) and acidified with 1% (v/v) HNO$_3$. The CDs samples were calibrated with a four-point calibration using the nutrient solution and samples were analyzed using the same spectrophotometer settings stated above. Iron levels

estimated with the CDs were confirmed using a Shimadzu Inductively Coupled Plasma Optical Emission Spectrometer (ICP-OES) 9810 (Kyoto, Japan). The system was calibrated using a five-point calibration and solution standards ranging from 2 to 10 ppm. Both calibration standards and hydroponic samples were acidified using HNO$_3$ (0.1 M) and analyzed at 238.39 nm. The hydroponic samples were filtered using a 0.2 μm SFCA syringe filter (Corning, AZ, USA) before ICP-OES analysis.

Data analysis

All measurements were performed in triplicate and the results are expressed as mean ± standard deviation. The data were submitted to t-test or analysis of variance (ANOVA) at a level of significance of 5% ($\alpha = 0.05$) using JMP Pro v.15 statistical software (SAS Institute, Cary, NC, USA). When necessary, significantly different means ($p < 0.05$) were separated by Tukey's Honest Significant Difference (HSD). Chi-square and fluorescent lifetime analysis were performed using Horiba EzTime software (Horiba, Ltd, Kyoto, Japan). The limit of detection (LOD) was calculated using the 3σ method[35] and the Stern–Volmer constant (K_{sv})[36] was the slope of the calibration curve.

Results and discussion

Material characterization

Size and morphology of the CDs were studied using transmission electron microscopy (TEM) with imaged particles (Fig. 1a and b) showing a mostly dispersed quasi-spherical structure with sizes ranging from 2 to 5 nm and an average size of 3.19 ± 0.76 nm. This size range is similar for recent work with CDs produced by microwave assisted methods.[37,38] The inset in Fig. 1b shows the lattice fringes of an imagined particle with an estimated lattice spacing of 0.26 nm corresponding to (100) facets of graphite.[39–41] Fig. 1c shows a selected area diffraction (SAED) image with large continuous diffuse rings indicating an amorphous nature of the bulk solution.[42–44]
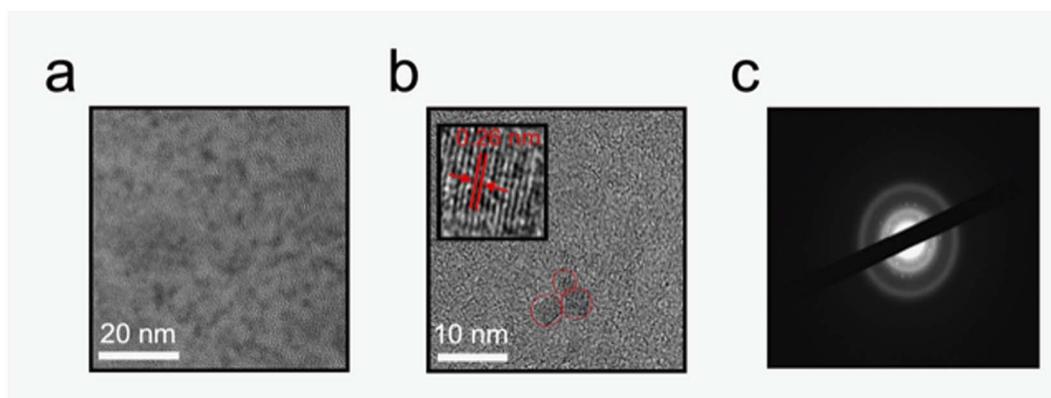

Fig. 1 (a) TEM image of the CDs showing semi-dispersed nanoparticles. (b) Additional TEM image of three CDs (red circles) displaying the quasi-spherical shape. The inset shows the lattice spacing of 0.26 nm corresponding to the (100) facets of graphite. (c) SAED image with large diffuse rings indicating an amorphous structure for the CDs.
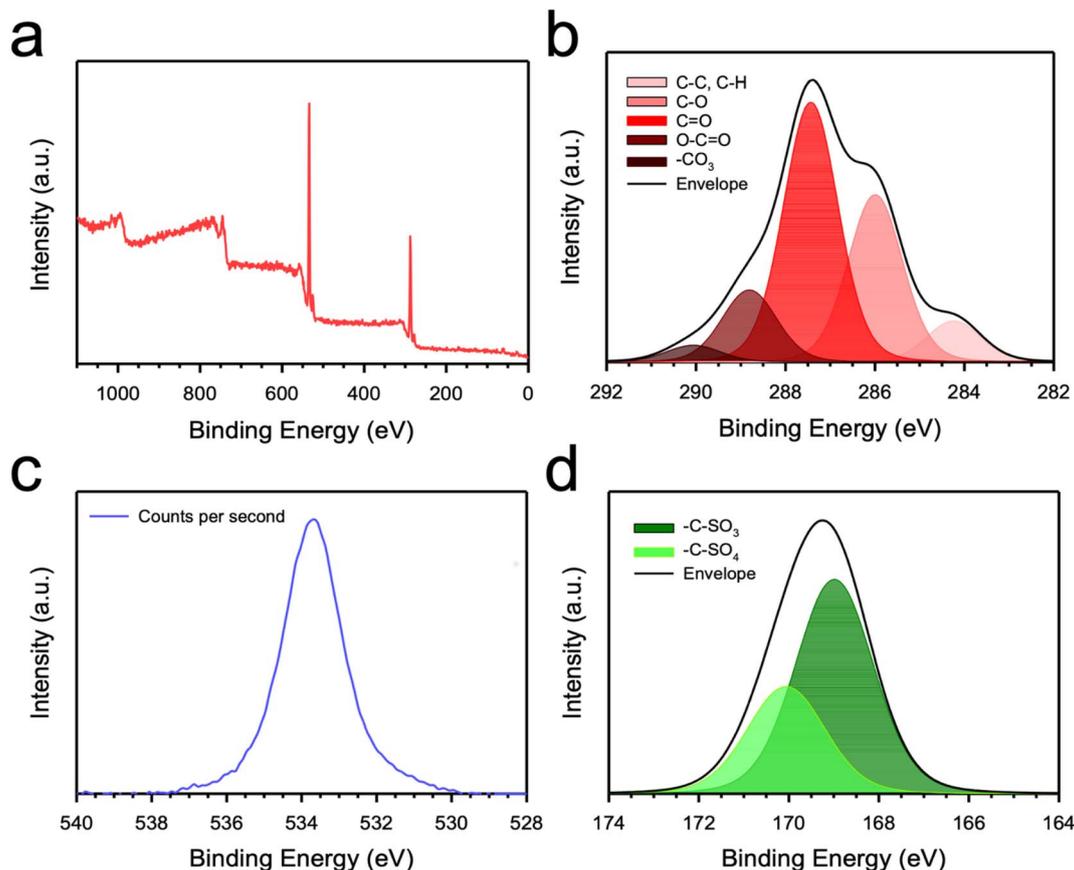
© 2023 The Author(s). Published by the Royal Society of Chemistry

Fig. 2 (a) XPS survey showing peaks at 287.4 eV and 533.7 eV attributed to the C1s and O1s, respectively. (b) Deconvoluted C1s peak showing the various carbon–oxygen and carbon–hydrogen groups present on the CDs surface. (c) Deconvoluted O1s peak at approximately 533.7 eV. (d) Deconvoluted S(2p) groups showing the small but present amount of sulfur groups on the CDs surface. The total XPS analysis resulted in 62.4% carbon, 36.5% oxygen, and 1.1% sulfur.

The surface composition of the CDs was studied with X-ray photoelectron spectroscopy (XPS) (Fig. 2a–d) and resulted in 62.4% carbon, 36.5% oxygen, and 1.1% sulfur which is likely from the surfactant sodium dodecylbenzene sulfonate present in Windex®.[45] Two peaks appear at 287.4 eV and 533.7 eV attributed to C1s and O1s, respectively. The C1s can be deconvoluted into five different peaks centered at 284.2, 286.0, 287.4, 288.8, 290.1 eV corresponding to C–C, C–O, C=O, O–C=O, and –CO$_3$ bonds, respectively, indicating a carbon core structure with predominantly oxygen surface groups. The high degree of oxygen groups is likely from the glycol ether cleaning agent[45] in Windex®, as similar result have been published using ethylene glycol as a dopant. Raman spectroscopy is often employed to study graphene or graphite-based material by observing the intensities of the D peak (typically ~1350 cm^{-1} and indicating disorder) and G peak (typically ~1580 cm^{-1} and indicating the degree of graphitization).[46,47] However, due to the strong fluorescent interference from the CDs, no meaningful Raman spectroscopy results were obtained for this study.

Optical properties

The optical properties of the CDs were studied first by UV-vis adsorption shown in Fig. 3a. A broad adsorption peak is observed at ~286 nm, which is attributed to the n–π* transitions of the C=O bonds and the π–π* transitions of the aromatic sp^2 carbons (aromatic C=C bonds).[48,49] The fluorescence lifetime (Fig. 3b) was measured by a time correlated single photon counting (TCSPC) fluorometer. Deconvolution analysis of the lifetime measurements was done using Horiba EzTime software and was interpreted using eqn (3). A three-component decay model was fit to the curve ($\chi^2 = 1.06$) and provided the following lifetimes: $\tau_1 = 2.71 \pm 0.21$ ns (42.02%), $\tau_2 = 9.02 \pm 0.20$ ns (33.18%), $\tau_3 = 0.63 \pm 0.03$ ns (24.80%), and $\tau_{avg} = 1.71 \pm 0.30$ ns. τ_2 is attributed to the electronic transitions in the surface state or defect sites, while τ_1 and τ_3 are attributed to electronic transitions in the carbon core.[50] The CDs exhibited cyan colored emission at approximately 500 nm when excited at 405 nm (Fig. 3c). The CDs showed excitation-dependance as the emission becomes slightly redshifted with increases in excitation wavelength from 345 to 425 nm. Further, when the excitation was below 375 nm a bimodal peak was observed. It is evident from Fig. 3c that the maximum emission peak is displayed when particles were excited at 405 nm (dark red curve), therefore, this excitation wavelength was used for subsequent quenching experiments.
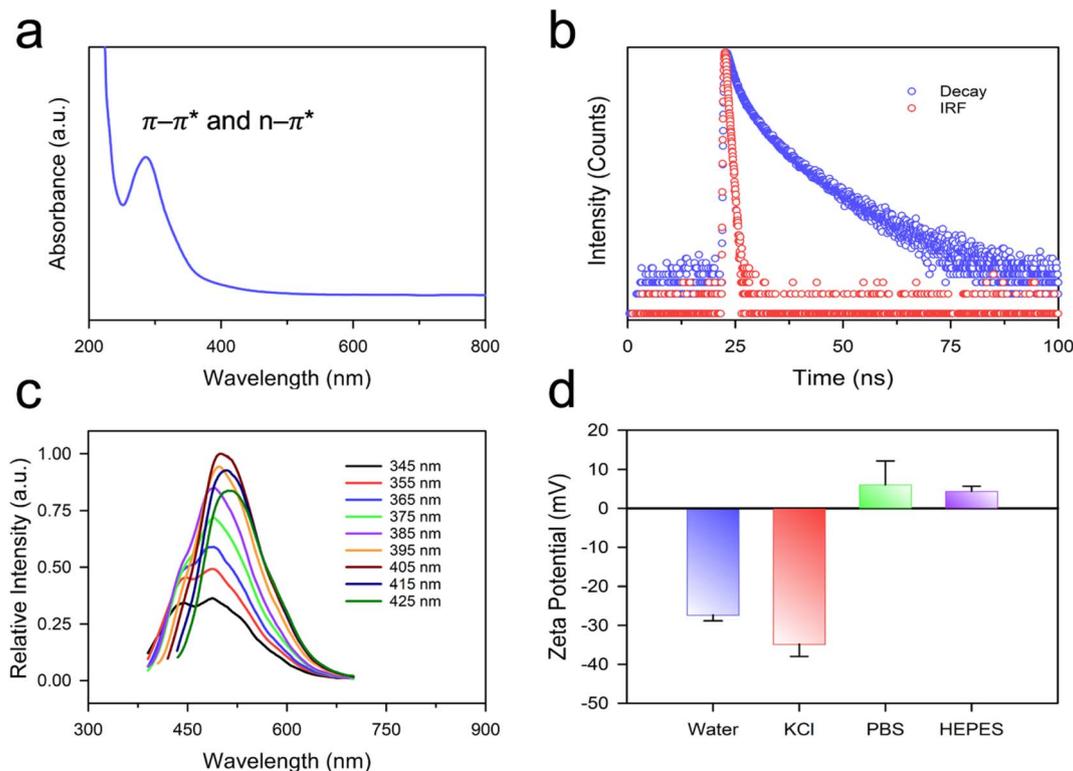
Fig. 3 (a) Absorbance spectra of the CDs showing a peak at ~286 nm likely due to n−π* and π−π* transitions. (b) Photoluminescence decay profile of the CDs giving an average lifetime of 1.71 ± 0.30 ns (blue curve) and the instrument response function (IRF, red curve). (c) Fluorescent emission peaks at various excitation wavelengths spanning from 345 to 425 nm showing the highest peak emission at excitation 405 nm (dark red curve). (d) Zeta potential measurements in water (blue bar), KCl (red bar), PBS (green bar), and HEPES buffer (purple bar).

The surface charge of the CDs was studied using zeta potential (ζ) measurements in water, 1 mM KCl, 1 mM PBS, and 1 mM HEPES (Fig. 3d). For measurements in water and KCl, the CDs displayed a negative zeta potential of -27.31 ± 1.52 mV and -34.79 ± 3.18 mV, respectively, which is advantageous for storage and long-term use of the CDs due to the electrostatic repulsion and consequently preventing agglomeration.[51,52] This was further confirmed by the minimal difference between peak emission from freshly prepared CDs and CDs stored in a dark drawer for one and two years (Fig. S3†). The zeta potential for CDs in the two buffers, PBS and HEPES, was 6.07 ± 6.11 mV and 4.40 ± 1.30 mV, respectively. The negative charge in water and 1 mM KCl is likely due to the presence of negatively charged oxygen groups, which are protonated in the two buffers leading to the large shift in ζ.[53,54]

Fluorescent quantum yield (QY) is a common characterization of fluorescent materials and is typically defined as the number of photons emitted per photons absorbed.[34] The CDs displayed a modest QY of ~13.0% against the standard of fluorescein (5 ppm, QY ~ 89% in 0.1 M NaOH). QY measurements are highly dependent on the method and conditions during testing (*e.g.*, standards and excitation wavelengths used for measurements); however, the CDs here displayed similar QY when compared to other fabrication methods (QY typically range from 3 to 30% for CDs).[17,55] Some groups have recently reported producing highly efficient CDs, with QY ranging from ~70–90%.[56–58]

The pH of hydroponic solutions affects the availability of certain nutrients. A lower pH (*e.g.*, 5.5) will keep most nutrients in solution while a higher pH (*e.g.*, >6.5) is likely to cause nutrient deprivation.[59] Temperature is another influential factor in hydroponic growing operations, and is tightly controlled with previous studies showing optimal growing temperature (*i.e.*, air and solution temperature) being 24 °C.[60] The effect of pH at 25 °C on the fluorescence of the CDs was studied at pH levels of 5.5 and 6.5 along with a high pH (7.9) to determine any dependence of the photoluminescence on pH levels. As shown in Fig. S2,† a non-significant difference ($p > 0.05$) in peak emission was observed for all pH levels tested. The minimal effect for relevant pH levels at 25 °C, show the CDs produced in this study are well-suited for iron detection in hydroponic growing operations.

Quenching of CDs fluorescence

Quenching of the CDs fluorescence was demonstrated in the presence of Fe^{3+} ions, as shown in Fig. 4a. Moreover, the quenching follows the Stern–Volmer equation[36] (eqn (1)).

A linear relationship is observed from approximately 0.14–11.17 ppm (Fig. 4b) with a calculated LOD of 0.196 ± 0.067 ppm (3.51 ± 1.21 μM) using the 3σ method, and an average Stern–Volmer constant (K_{sv}) of 0.0052/ppm-Fe^{3+}. The quenching induced by the Fe^{3+} ions is likely due to coordinate bonding of the Fe^{3+} ions with the oxygen surface groups of the CDs.[61] The
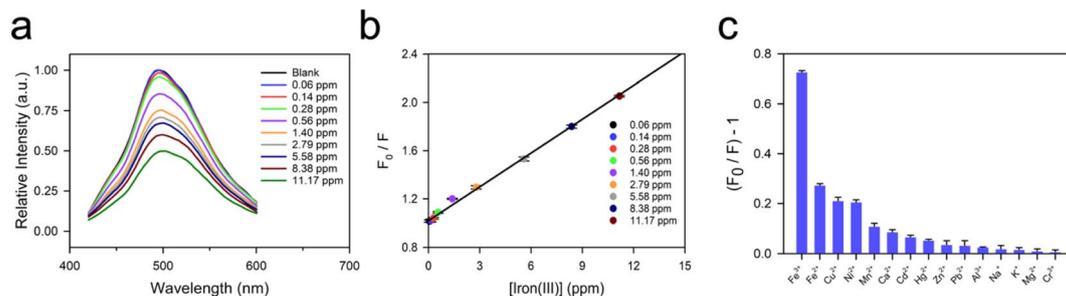
Fig. 4 (a) Fluorescent quenching of the CDs in the presence of ferric iron with concentrations ranging from 0.06 to 11.17 ppm. (b) Stern–Volmer plot displaying the linear ($R^2 = 0.9972$) quenching of the CDs by ferric iron with a K_{sv} value of 0.0052/ppm-Fe^{3+} and an LOD of 0.196 ± 0.067 ppm (3.51 ± 1.21 μM). (c) Selectivity testing of the CDs using common heavy metal quenchers of CDs and various cations present in hydroponic solutions displaying minimal quenching from interfering cations and high selectivity towards ferric iron. Data represents mean ± standard deviation ($n = 3$).

LOD is quite high when compared to recently published work on ferric iron sensing with CDs,[62–65] however, the LOD is still below the Environmental Protection Agency (EPA) limit of iron in drinking water (0.3 mg L^{-1})[66] and is well within the range commonly used in hydroponic systems (~1–2 ppm),[67,68] which demonstrates the value of the proposed technology in agricultural applications. Fourteen cations were selected to test the selective quenching ability of the CDs for Fe^{3+} including Pb^{2+}, Zn^{2+}, Hg^{2+}, Cd^{2+}, Ca^{2+}, Mn^{2+}, Ni^{2+}, Cr^{3+}, Al^{3+}, Cu^{2+}, Mg^{2+}, K^+, Na^+, and Fe^{2+} (100 μM). As shown in Fig. 4c, Ni^{2+}, Cu^{2+}, and Fe^{2+} induced a slight quenching of the CDs fluorescence but was still considerably lower than the quenching induced by Fe^{3+} while the remaining cations induced negligible effects on the fluorescence of the CDs.

The form of quenching (static or dynamic) can be determined by measuring fluorescent lifetimes and absorbance spectra.[69]

During static quenching, the CDs form a nonfluorescent complex with the quencher. This is typically determined through observing changes in the absorbance spectra with no changes in the fluorescent lifetime in the presence and absence of a quencher.[70] Dynamic quenching refers to the collisional or close-contact quenching of CDs fluorescence facilitating energy transfer and allowing a non-radiative return to the ground state.[70] This typically results in changes of the fluorescent lifetime in the presence of a quencher while no observable changes in the absorbance spectra are detected.[70] Absorbance and fluorescent lifetime data were collected in the presence and absence of the quencher with no changes occurring in the absorbance spectra but a reduction in the average fluorescent lifetime from 1.71 ns to 0.77 ns ($\chi^2 = 1.65$). These results support the dynamic quenching of the CDs fluorescence in the presence of ferric iron.
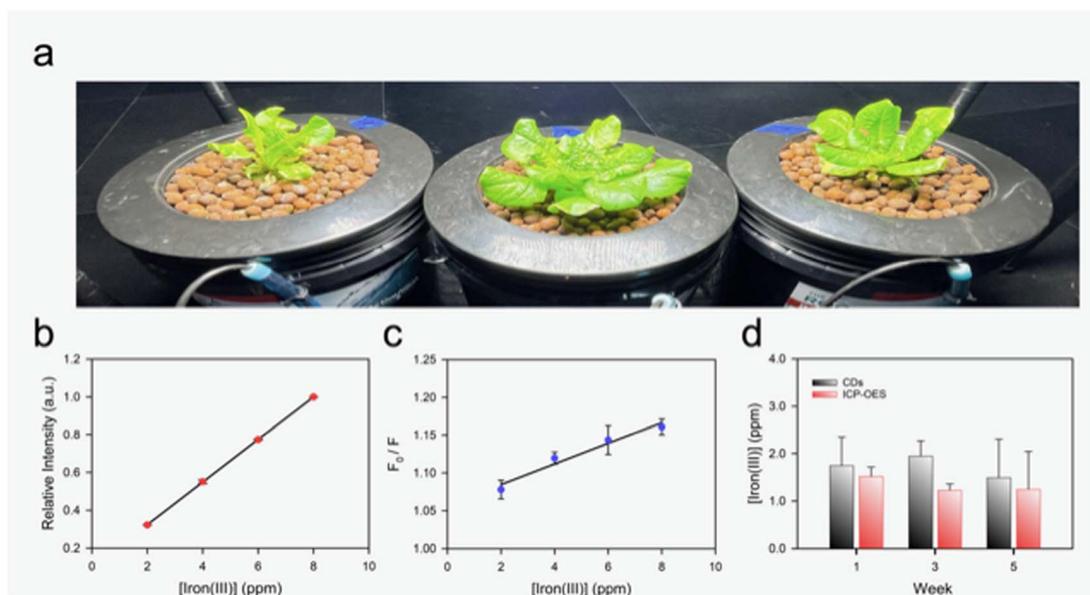

Fig. 5 (a) Series of DWC hydroponic set-ups used to grow lettuce. (b) ICP-OES calibration curve ($R^2 = 0.9999$) using the hydroponic nutrient solution for testing. (c) CDs calibration curve ($R^2 = 0.9992$) using the hydroponic nutrient solution for testing. (d) Results for both CDs (black bars) and ICP-OES (red bars) using hydroponic samples from week one, three, and five of plant growth showing a non-significant difference ($p > 0.05$) between ICP-OES and CDs performance in Fe^{3+} quantification. Data represents mean ± standard deviation ($n = 3$).

Hydroponic sample testing

A series of three deep-water culture (DWC) hydroponic systems (Fig. 5a) were used to grow butterhead lettuce (*Lactuca sativa* var. *capitata* L.) to test the CDs in real samples. DWC water samples were collected during weeks one, three, and five of growth and analyzed on the same day with a calibrated ICP-OES (calibration Fig. 5b, sample analysis Fig. 5d red bars). CDs were prepared and calibrated with the nutrient solution using a four-point calibration from 2.5 to 10 ppm (Fig. 5c). The collected DWC water samples were acidified with 1% (v/v) HNO_3 before analysis with the CDs and analyzed on the same day (Fig. 5d black bars). For all samples over the three sampling times, representing start, middle-point, and end of lettuce cultivation, the CDs displayed a non-significant difference in iron concentration when compared to the ICP-OES analysis ($p > 0.05$).

These results demonstrate the CDs ability to act as inexpensive (~$0.03 of material costs (Windex® and glucose) per analysis with ~12 sample analysis per batch) iron sensor for hydroponic systems. Potential combination of the CDs in this study with a portable spectrophotometer[71,72] could provide the ability for growers or researchers to perform iron quantification on-site significantly reducing analysis time for nutrient monitoring. Using a portable spectrophotometer (Vernier spectrophotometer, Ocean Optics Inc., Florida, USA) equipped with a fiber optic cable (P400-2-UV-VIS, Ocean Optics Inc., Florida, USA) a broad emission peak centered around 550 nm is observed. Quenching of the fluorescence in the presence of ferric iron was also observed with the portable set-up demonstrating the ability to mobilize the sensing platform (Fig. S4†). In the future, the CDs could also be developed into colorimetric test strips, such as those used to measure pH, to facilitate easier and lower cost analysis of hydroponic samples.[73–75] Furthermore, some groups have demonstrated the ability to attach specific recognition agents to the surface of CDs, which could potentially be used to design a complete system for monitoring ions relevant to hydroponic farming.[76]

Conclusions

Hydroponic growers typically use electrical conductivity or total dissolved salts measurements to estimate nutrient levels in their growing systems. These methods, while rapid, do not provide the grower any insight on particular nutrient levels causing growers to apply all relevant nutrients when deficiencies arise or apply nutrients in a time-based manner. Selective, sensitive, and user-friendly rapid sensors for relevant nutrients are needed to support precision agriculture efforts to accurately determine what particular nutrient is deficient or in excess, thus increasing their productivity and reducing their overhead cost. Such a sensing system would also allow researchers insight on nutrient mobility and uptake by plants leading to better understanding, and potentially more control, of plant growth in hydroponic systems. Iron is one of the most important micronutrients to plant health and lacks inexpensive, rapid, and portable sensors that are useable in hydroponics. In this study, CDs were produced with a standard

household microwave, glucose, and Windex® with ~1 min pyrolysis time. The CDs were then applied to accurately monitor ferric iron (Fe^{3+}) in water samples from a DWC hydroponic system where butterhead lettuce was grown. The CDs were able to accurately measure iron levels during three separate weeks of growth with a non-significant ($p > 0.05$) difference in performance when compared to analysis with ICP-OES. The calculated LOD was 0.196 ± 0.067 ppm (3.51 ± 1.21 µM) with a linear response from 0.14 to 11.17 ppm, which is well-within the typical concentration ranges for iron in hydroponic systems. Furthermore, the CDs demonstrated high selectivity to iron with minimal quenching from other cations present in hydroponic solutions and common heavy metals quenchers. The simple production and accurate sensing capabilities of the CDs make them appealing for the development of iron monitoring in hydroponic systems.

Conflicts of interest

The authors declare no competing financial interest.

Acknowledgements

References

1 P. A. Frey and G. H. Reed, *ACS Chem. Biol.*, 2012, **7**, 1477–1481.

2 N. Abbaspour, R. Hurrell and R. Kelishadi, *Review on iron and its importance for human health*, 2014.

3 Y. Zuo and F. Zhang, *Plant Soil*, 2011, **339**, 83–95.

4 B. de Benoist, World Health Organization and Centers for Disease Control and Prevention (U.S.), *Worldwide prevalence of anaemia 1993-2005 of: WHO Global Database of anaemia*, World Health Organization (WHO), 2020.

5 J. F. Ma and H. Q. Ling, *Plant Soil*, 2009, **325**, 1–3.

6 H. Singh, G. Assistant and V. Dunn Bruce, *Electrical Conductivity and pH Guide for Hydroponics*, 2016.

7 G. v. Sandoya, J. Bosques, F. Rivera and E. V. Campoverde, *EDIS*, 2021, DOI: 10.32473/edis-hs1422-2021.

8 J. E. Son, H. J. Kim and T. I. Ahn, in *Plant Factory*, Elsevier, 2nd edn, 2020, pp. 273–283.

9 M. T. Ko, T. I. Ahn, Y. Y. Cho and J. E. Son, *Hortic., Environ. Biotechnol.*, 2013, **54**, 412–421.

10 X. Xu, R. Ray, Y. Gu, H. J. Ploehn, L. Gearheart, K. Raker and W. A. Scrivens, *J. Am. Chem. Soc.*, 2004, **126**, 12736–12737.

11 H. Li, Z. Kang, Y. Liu and S. T. Lee, *J. Mater. Chem.*, 2012, **22**, 24230–24253.

12 J. Zhang and S. H. Yu, *Mater. Today*, 2016, **19**, 382–393.

13 Y. Wang and A. Hu, *J. Mater. Chem. C*, 2014, **2**, 6921–6939.

14 J. Joseph and A. A. Anappara, *ChemPhysChem*, 2017, **18**, 292–298.

15 Z. Guo, J. Luo, Z. Zhu, Z. Sun, X. Zhang, Z. chao Wu, F. Mo and A. Guan, *Dyes Pigm.*, 2020, **173**, 107952.

16 S. C. Ray, A. Saha, N. R. Jana and R. Sarkar, *J. Phys. Chem. C*, 2009, **113**, 18546–18551.

17 A. Tadesse, M. Hagos, D. Ramadevi, K. Basavaiah and N. Belachew, *ACS Omega*, 2020, **5**, 3889–3898.

18 Y. Liu, Y. Liu, M. Park, S. J. Park, Y. Zhang, M. R. Akanda, B. Y. Park and H. Y. Kim, *Carbon Lett.*, 2017, **21**, 61–67.

19 B. S. B. Kasibabu, S. L. D'souza, S. Jha, R. K. Singhal, H. Basu and S. K. Kailasa, *Anal. Methods*, 2015, **7**, 2373–2378.

20 H. Ding, S. B. Yu, J. S. Wei and H. M. Xiong, *ACS Nano*, 2016, **10**, 484–491.

21 S. Kang, Y. K. Jeong, J. H. Ryu, Y. Son, W. R. Kim, B. Lee, K. H. Jung and K. M. Kim, *Appl. Surf. Sci.*, 2020, **506**, 144998.

22 H. Li, J. Huang, Y. Song, M. Zhang, H. Wang, F. Lu, H. Huang, Y. Liu, X. Dai, Z. Gu, Z. Yang, R. Zhou and Z. Kang, *ACS Appl. Mater. Interfaces*, 2018, **10**, 26936–26946.

23 Y. Hou, Q. Lu, J. Deng, H. Li and Y. Zhang, *Anal. Chim. Acta*, 2015, **866**, 69–74.

24 S. Mitra, S. Chandra, T. Kundu, R. Banerjee, P. Pramanik and A. Goswami, *RSC Adv.*, 2012, **2**, 12129–12131.

25 T. V. De Medeiros, J. Manioudakis, F. Noun, J. R. Macairan, F. Victoria and R. Naccache, *J. Mater. Chem. C*, 2019, **7**, 7175–7195.

26 X. Wang, K. Qu, B. Xu, J. Ren and X. Qu, *J. Mater. Chem.*, 2011, **21**, 2445–2450.

27 Z. Zhang, J. Hao, J. Zhang, B. Zhang and J. Tang, *RSC Adv.*, 2012, **2**, 8599–8601.

28 V. N. Mehta, S. Jha, H. Basu, R. K. Singhal and S. K. Kailasa, *Sens. Actuators, B*, 2015, **213**, 434–443.

29 Z. C. Yang, M. Wang, A. M. Yong, S. Y. Wong, X. H. Zhang, H. Tan, A. Y. Chang, X. Li and J. Wang, *Chem. Commun.*, 2011, **47**, 11615–11617.

30 S. Huang, W. Li, P. Han, X. Zhou, J. Cheng, H. Wen and W. Xue, *Anal. Methods*, 2019, **11**, 2240–2258.

31 M. Li, T. Chen, J. J. Gooding and J. Liu, *ACS Sens.*, 2019, **4**, 1732–1748.

32 A. S. Rasal, S. Yadav, A. Yadav, A. A. Kashale, S. T. Manjunatha, A. Altaee and J. Y. Chang, *ACS Appl. Nano Mater.*, 2021, **4**, 6515–6541.

33 M. J. Molaei, *Anal. Methods*, 2020, **12**, 1266–1287.

34 C. Würth, M. Grabolle, J. Pauli, M. Spieles and U. Resch-Genger, *Nat. Protoc.*, 2013, **8**, 1535–1550.

35 A. J. Cunningham, *Introduction to Bioanalytical Sensors*, Wiley-Interscience, 1st edn, 1998.

36 H. Boaz and G. K. Rollefson, *J. Am. Chem. Soc.*, 1950, **72**, 3435–3443.

37 S. Bhattacharyya, F. Ehrat, P. Urban, R. Teves, R. Wyrwich, M. Döblinger, J. Feldmann, A. S. Urban and J. K. Stolarczyk, *Nat. Commun.*, 2017, **8**(1), 1401.

38 A. Pathak, S. Pv, J. Stanley and T. G. Satheesh Babu, *Microchim. Acta*, 2019, **186**(3), 157.

39 Y. Wei, L. Chen, J. Wang, X. Liu, Y. Yang and S. Yu, *RSC Adv.*, 2019, **9**, 3208–3214.

40 L. Li, Y. Li, Y. Ye, R. Guo, A. Wang, G. Zou, H. Hou and X. Ji, *ACS Nano*, 2021, **15**, 6872–6885.

41 H. J. Yoo, B. E. Kwak and D. H. Kim, *J. Phys. Chem. C*, 2019, **123**, 27124–27131.

42 Y. Zheng, D. Yang, X. Wu, H. Yan, Y. Zhao, B. Feng, K. Duan, J. Weng and J. Wang, *RSC Adv.*, 2015, **5**, 90245–90254.

43 P. M. Krishna, V. Polisetti, K. Damarla, S. K. Mandal and A. Kumar, *RSC Adv.*, 2021, **11**, 21207–21215.

44 V. Arul and M. G. Sethuraman, *ACS Omega*, 2019, **4**, 3449–3457.

45 S. C. Johnson, *Windex Original Glass Cleaner*, https://www.whatsinsidescjohnson.com/us/en/brands/windex/windex-original-glass-cleaner, accessed 15 December 2022.

46 J. Zhan, R. Peng, S. Wei, J. Chen, X. Peng and B. Xiao, *ACS Omega*, 2019, **4**, 22574–22580.

47 R. G. Hjort, R. R. A. Soares, J. Li, D. Jing, L. Hartfiel, B. Chen, B. van Belle, M. Soupir, E. Smith, E. Mclamore, J. C. Claussen and C. L. Gomes, *Microchim. Acta*, 2022, 1–11.

48 L. Zhao, F. Di, D. Wang, L. H. Guo, Y. Yang, B. Wan and H. Zhang, *Nanoscale*, 2013, **5**, 2655–2658.

49 X. Jia, J. Li and E. Wang, *Nanoscale*, 2012, **4**, 5572–5575.

50 Y. Ding, J. Zheng, J. Wang, Y. Yang and X. Liu, *J. Mater. Chem. C*, 2019, **7**, 1502–1509.

51 J. Zhou, H. Zhou, J. Tang, S. Deng, F. Yan, W. Li and M. Qu, *Microchim. Acta*, 2017, **184**, 343–368.

52 H. Rao, H. Ge, X. Wang, Z. Zhang, X. Liu, Y. Yang, Y. Liu, W. Liu, P. Zou and Y. Wang, *Microchim. Acta*, 2017, **184**, 3017–3025.

53 A. Verma, F. Arshad, K. Ahmad, U. Goswami, S. K. Samanta, A. K. Sahoo and M. P. Sk, *Nanotechnology*, 2020, **31**(9), 095101.

54 X. W. Hua, Y. W. Bao, H. Y. Wang, Z. Chen and F. G. Wu, *Nanoscale*, 2017, **9**, 2150–2161.

55 H. Ehtesabi, Z. Hallaji, S. Najafi Nobar and Z. Bagheri, *Microchim. Acta*, 2020, **187**(2), 150.

56 Ö. K. Koç, A. Üzer and R. Apak, *ACS Appl. Nano Mater.*, 2022, **5**, 5868–5881.

57 Y. Wu, D. Qin, Z. Luo, S. Meng, G. Mo, X. Jiang and B. Deng, *ACS Sustainable Chem. Eng.*, 2022, **10**, 5195–5202.

58 H. Liu, Z. Li, Y. Sun, X. Geng, Y. Hu, H. Meng, J. Ge and L. Qu, *Sci. Rep.*, 2018, **8**(1), 1086.

59 T. S. Anderson, M. R. Martini, D. de Villiers and M. B. Timmons, *Horticulturae*, 2017, **3**(3), 41.

60 H. C. Thompson, R. W. Langhans, A.-J. Both and L. D. Albright, *J. Am. Soc. Hortic. Sci.*, 1998, **123**, 361–364.

61 X. Gong, W. Lu, M. C. Paau, Q. Hu, X. Wu, S. Shuang, C. Dong and M. M. F. Choi, *Anal. Chim. Acta*, 2015, **861**, 74–84.

62 Y. Wu, L. Cao, M. Zan, Z. Hou, M. Ge, W. F. Dong and L. Li, *Analyst*, 2021, **146**, 4954–4963.

63 S. H. K. Yap, K. K. Chan, G. Zhang, S. C. Tjin and K. T. Yong, *ACS Appl. Mater. Interfaces*, 2019, **11**, 28546–28553.

64 R. Sinha, A. P. Bidkar, R. Rajasekhar, S. S. Ghosh and T. K. Mandal, *Can. J. Chem. Eng.*, 2020, **98**, 194–204.

65 S. K. Kailasa, S. Ha, S. H. Baek, L. M. T. Phan, S. Kim, K. Kwak and T. J. Park, *Mater. Sci. Eng., C*, 2019, **98**, 834–842.

66 United States Environmental Protection Agency, *2018 Edition of the Drinking Water Standards and Health Advisories Tables*, 2018.

67 T. Ford, R. Berghage, F. di Gioia and N. Flax, *Hydroponics Systems: Nutrient Solution Programs and Recipes*, 2022.

68 N. S. Mattson and C. Peters, *Inside Grower*, 2014, 16–19.

69 F. Noun, E. A. Jury and R. Naccache, *Sensors*, 2021, **21**, 1–13.

70 F. Zu, F. Yan, Z. Bai, J. Xu, Y. Wang, Y. Huang and X. Zhou, *Microchim. Acta*, 2017, **184**, 1899–1914.

71 S. Srivastava and V. Sharma, *Appl. Water Sci.*, 2021, **11**(11), 177.

72 J. J. Poh, W. L. Wu, N. W. J. Goh, S. M. X. Tan and S. K. E. Gan, *Sens. Actuators, A*, 2021, **325**, 112698.

73 R. B. Alnoman, S. D. Al-Qahtani, A. Bayazeed, A. M. Munshi, A. Alsoliemy, S. A. Alqarni and N. M. El-Metwaly, *ACS Omega*, 2022, **7**, 5595–5604.

74 Y. Song, X. Wang, H. Liu, X. Wang, D. Li, H. L. Zhu and Y. Qian, *Talanta*, 2022, **246**, 123366.

75 Q. Chen, Y. Sun, S. Liu, J. Zhang, C. Zhang, H. Jiang, X. Han, L. He, S. Wang and K. Zhang, *Sens. Actuators, B*, 2021, **344**.

76 M. Yang, C. Liu, Y. Peng, R. Z. Xiao, S. Zhang, Z. L. Zhang, B. Zhang and D. W. Pang, *Anal. Chim. Acta*, 2021, **1146**, 33–40.